Molecular Biology of the Cell
Vol. 15, 5001–5011, November 2004

Roles of the Mammalian Mitochondrial Fission and Fusion Mediators Fis1, Drp1, and Opa1 in Apoptosis

Yang-ja Lee,*† Seon-Yong Jeong,*† Mariusz Karbowski,* Carolyn L. Smith,‡ and Richard J. Youle*§

*Biochemistry Section, Surgical Neurology Branch, and ‡Light Imaging Facility, National Institute of Neurological Disorders and Stroke, National Institutes of Health, Bethesda, MD 20892

Submitted April 8, 2004; Revised August 5, 2004; Accepted August 30, 2004
Monitoring Editor: Keith Yamamoto

During apoptosis, the mitochondrial network fragments. Using short hairpin RNAs for RNA interference, we manipulated the expression levels of the proteins hFis1, Drp1, and Opa1 that are involved in mitochondrial fission and fusion in mammalian cells, and we characterized their functions in mitochondrial morphology and apoptosis. Down-regulation of hFis1 powerfully inhibits cell death to an extent significantly greater than down-regulation of Drp1 and at a stage of apoptosis distinct from that induced by Drp1 inhibition. Cells depleted of Opa1 are extremely sensitive to exogenous apoptosis induction, and some die spontaneously by a process that requires hFis1 expression. Wild-type Opa1 may function normally as an antiapoptotic protein, keeping spontaneous apoptosis in check. However, if hFis1 is down-regulated, cells do not require Opa1 to prevent apoptosis, suggesting that Opa1 may be normally counteracting the proapoptotic action of hFis1. We also demonstrate in this study that mitochondrial fragmentation per se does not result in apoptosis. However, we provide further evidence that multiple components of the mitochondrial morphogenesis machinery can positively and negatively regulate apoptosis.

INTRODUCTION

Mitochondria are morphologically dynamic organelles that continuously divide and fuse to form small individual units or interconnected networks within the cell (Bereiter-Hahn, 1990). They reach an equilibrium between these two states in healthy cells by regulating the relative rates of organelle fusion and fission (Nunnari *et al*., 1997). Proteins controlling mitochondrial fission include Drp1 (*DNM1* in yeast) (Otsuga *et al*., 1998; Bleazard *et al*., 1999), Fis1 (Mozdy *et al*., 2000; Jakobs *et al*., 2003), and up to six other gene products in yeast (Dimmer *et al*., 2002). Drp1 is a large GTPase similar to dynamin, a protein that spirals around the necks of endocytic vesicles and facilitates their scission from the plasma membrane (Hinshaw, 2000). Inhibition of Drp1 GTPase activity with a dominant negative protein defective in GTP binding ($Drp1^{K38A}$) results in elongated mitochondria, confirming that in mammalian cells (Smirnova *et al*., 1998, 2001; Frank *et al*., 2001) Drp1 functions like its yeast ortholog *DNM1* in mitochondrial fission (Otsuga *et al*., 1998; Bleazard *et al*., 1999). Drp1 exists primarily in the cytoplasm but partially associates into foci on the outer surface of mitochondria that coalesce at sites of organelle fission (Smirnova *et al*., 2001). Human Fis1 (hFis1) contains a tetratricopeptide repeat (TPR) motif domain (Suzuki *et al*., 2003; Dohm *et al*., 2004) facing the cytoplasm and is anchored in the outer mitochondrial membrane via a C-terminal hydrophobic tail (Yoon *et al*., 2003). hFis1 circumscribes the outer surface of mitochondria and is not localized specifically to mitochondrial scission sites (Suzuki *et al*., 2003; Yoon *et al*., 2003). Down-regulating mammalian Fis1 expression by RNA interference (RNAi) induces mitochondrial elongation (Stojanovski *et al*., 2004), confirming results previously reported in yeast that *FIS1* is involved in mitochondrial fission (Mozdy *et al*., 2000; Jakobs *et al*., 2003).

Mitochondrial fusion in mammalian cells is controlled by the large GTPases Mfn1 (Santel and Fuller, 2001; Ishihara *et al*., 2003), Mfn2 (Santel and Fuller, 2001; Ishihara *et al*., 2003), and Opa1 (*MGM1* in yeast) (Olichon *et al*., 2002; Satoh *et al*., 2003). Elimination of any of these proteins induces mitochondrial fragmentation (Chen *et al*., 2003; Olichon *et al*., 2003; Griparic *et al*., 2004). Mutations in Opa1 were found to cause dominant optic atrophy (Alexander *et al*., 2000; Delettre *et al*., 2000), potentially connecting this process (inhibition of mitochondrial fusion) to human disease.

During apoptosis, the mitochondrial network fragments, resulting in smaller and more numerous mitochondria (Mancini *et al*., 1997; De Vos *et al*., 1998; Zhuang *et al*., 1998; Desagher *et al*., 1999; Frank *et al*., 2001; Karbowski *et al*., 2002). It has been reported that increased fission, decreased fusion, or both cause this mitochondrial phenotype at a stage of apoptosis upstream of caspase activation and close to that of Bax translocation to mitochondria and cytochrome *c* release (Karbowski *et al*., 2004), suggesting a mechanistic link between mitochondrial morphology and apoptosis. Drp1 binding to mitochondria is increased during apoptosis (Frank *et al*., 2001; Breckenridge *et al*., 2003), and the Drp1 foci at mitochondrial scission sites colocalize with foci of Bax that occur on mitochondria during apoptosis (Karbowski *et*

Article published online ahead of print. Mol. Biol. Cell 10.1091/mbc.E04–04–0294. Article and publication date are available at www.molbiolcell.org/cgi/doi/10.1091/mbc.E04–04–0294.

† These authors contributed equally to this work.

§ Corresponding author. E-mail address: youler@ninds.nih.gov.

Abbreviations used: Act D, actinomycin D; PARP, poly(ADP-ribose) polymerase; RNAi, RNA interference; shRNA, short hairpin RNA; STS, staurosporine; zVAD-fmk, z-Val-Ala-Asp(OMe)-fluoromethyl ketone.

al., 2002). Inhibition of Drp1 GTPase activity with a dominant negative protein ($Drp1^{K38A}$) prevents the mitochondrial fragmentation seen during apoptosis and delays the process of cell death (Frank *et al*., 2001; Karbowski *et al*., 2002), suggesting that mitochondrial fission is a required step in apoptosis. Overexpression of hFis1 has been reported to induce apoptosis (James *et al*., 2003), also suggesting the involvement of mitochondrial fission in apoptosis. Down-regulation of Opa1 expression in cells by RNAi results in spontaneous cell apoptosis (Olichon *et al*., 2003), suggesting that the promotion of mitochondrial fusion by wild-type levels of Opa1 normally protects cells from apoptosis.

To further investigate the link between mitochondrial fission and apoptosis, we have explored the role of hFis1 in these processes. Using short hairpin RNAs (shRNAs) for RNAi (Paddison *et al*., 2002), we have down-regulated three proteins involved in mitochondrial morphology: Drp1, hFis1, and Opa1. Using this technique, we are able to manipulate the expression levels of the proteins and to characterize their functions in mitochondrial morphology and apoptosis. Down-regulation of hFis1 powerfully inhibits cell death by multiple pathways to an extent significantly greater than down-regulation of Drp1 and at a stage of apoptosis distinct from that induced by Drp1 inhibition. Cells depleted of Opa1 are extremely sensitive to exogenous apoptosis induction and spontaneously die by a process that requires hFis1 expression. Thus, multiple proteins that comprise the mitochondrial morphogenesis machinery can positively and negatively regulate apoptosis.

MATERIALS AND METHODS

Cell Culture, Transfection, DNA Constructs, and RNAi

HeLa cells (American Type Culture Collection, Manassas, VA) were cultured in complete DMEM supplemented with 10% heat-inactivated fetal calf serum, 100 U/ml penicillin, and 100 μg/ml streptomycin in 5% CO_2 at 37°C. Transfections of HeLa cells were performed using FuGENE 6 (Roche Diagnostics, Indianapolis, IN) according to the manufacturer's instructions. The cDNA for hFis1 (GenBank accession no. AF151893) was cloned by reverse transcription-polymerase chain reaction with total human RNA as template. cDNA for wild-type hFis1 (hFis1wt) and hFis1 lacking the C-terminal 30 residues (hFis1ΔC) was cloned into mammalian expression vectors pcDNA3.1 and pREP4. RNAi was performed using the sh-activated gene silencing system (Paddison *et al*., 2002). The plasmids expressing shRNAs were constructed by synthesizing two cDNA oligonucleotides bearing the target sequence, *Hind*III linker, and U6 terminator, annealing them and ligating them into BseRI and *Bam*HI sites of pSHAG-1 (Cold Spring Harbor Laboratory, Cold Spring, NY). For long-term (stable) suppression of gene expression by shRNA, the region encoding the U6 promoter and shRNA in pSHAG-1 was subcloned into the *Not*I and *Bam*HI sites of pREP4 (Invitrogen, Carlsbad, CA). The target sequences for the hFis1, Opa1, and Drp1 were as follows: 5′-GAGACGCGGGAGCCCACGGAGAACGCTCC-3′ for hFis1, 5′-GATGAAGTTATCAGTCTGAGCCAGGTTAC-3′ for Opa1, and 5′-TTCAATCCGTGATGAGTATGCTTTTCTTC-3′ for Drp1. The sequence for the control shRNA was 5′-TCGTACTCATAATCAGCTCTGCATACATC-3′, which targets Opa1 3′ end noncoding region and has no effect on silencing of Opa1 gene expression. One day after the transfection with these pREP4 constructs, HeLa cells were grown in DMEM containing 300 μg/ml hygromycin B for 2 d followed by 3–4 d in DMEM containing 50 μg/ml hygromycin B for the selection of transfectants.

Immunocytochemistry and Confocal Microscopy

Cells grown in two-well chamber slides were treated as indicated, fixed with 4% paraformaldehyde for 10 min, permeabilized with 0.2% Triton X-100 for 15 min, and then blocked with 2% bovine serum albumin for 1 h at room temperature (RT). Cells were probed with rabbit polyclonal anti-Bax (1:800; Upstate Biotechnology, Lake Placid, NY), mouse monoclonal anti-cytochrome *c* (1:800; BD Biosciences PharMingen), or mouse monoclonal anti-DLP1/Drp1 (1:100; BD Transduction Laboratories, Lexington, KY) overnight at 4°C followed by staining with goat anti-rabbit Alexa Fluor 594 (1:600; Molecular Probes, Eugene, OR) or goat anti-mouse Alexa Fluor 488 antibodies (1:600; Molecular Probes) for 2 h at RT. After washing, cells were mounted with SlowFade light antifade reagent (Molecular Probes) and analyzed by confocal microscopy. To visualize the mitochondria in living cells, 50 nM Mitotracker CMXRos (Molecular Probes) was added and incubated for 30 min before confocal microscopy. To analyze the mitochondrial membrane potential, cells were incubated for 20 min with 5 μg/ml JC1 (Molecular Probes) in culture medium and observed by confocal microscopy. Images were captured with an LSM 510 Zeiss confocal microscope. Matrix-targeted photoactivable green fluorescent protein (mito-PAGFP)–based mitochondrial fusion assay was performed as described previously (Karbowski *et al*., 2004)

Subcellular Fractionation and Immunoblotting

Cells were permeabilized with digitonin (300 μg/ml) in cytosolic extraction buffer (250 mM sucrose, 70 mM KCl, 137 mM NaCl, 4.3 mM Na_2HPO_4, 1.4 mM KH_2PO_4, pH 7.2, 100 μM phenylmethylsulfonyl fluoride [PMSF], 10 μg/ml leupeptin, 2 μg/ml aprotinin) for 5 min on ice. Plasma membrane permeabilization of cells was confirmed by staining cells with trypan blue. Permeabilized cells were centrifuged at 1000 $\times$ *g* for 5 min at 4°C. The supernatants (cytosolic fractions; S) were saved, and the pellets were solubilized in the same volume of mitochondrial lysis buffer (50 mM Tris-Cl, pH 7.4, 150 mM NaCl, 2 mM EDTA, 2 mM EGTA, 0.2% Triton X-100, 0.3% NP-40, 100 μM PMSF, 10 μg/ml leupeptin, 2 μg/ml aprotinin), followed by centrifugation at 10,000 $\times$ *g* for 10 min at 4°C, and the supernatants were used as heavy membrane (HM) fractions. Total cell lysates were prepared by solubilizing whole cells in Laemmli sample buffer and boiling them for 10 min. An aliquot of each sample was taken to determine protein concentrations by BCA protein assay kit (Pierce Chemical, Rockford, IL). Equal amounts of samples were run on 4–12% polyacrylamide gradient gels (Invitrogen), transferred to polyvinylidene difluoride membranes (Immobilon-P; Millipore, Billerica, MA), and immunoblotted. The primary antibodies, their dilutions, and their sources are as follows: anti-Fis1 (1:500; Axxora, San Diego, CA), anti-Opa1 (Zhu *et al*., 2003), anti-DLP1/Drp1 (1:1000; BD Transduction Laboratories), anti-Bax (1:1000; Santa Cruz Biotechnology), anti-cytochrome *c* (1:1000; BD Biosciences PharMingen), anti-PARP (1:1000; BIOMOL Research Laboratories, Plymouth Meeting, PA), and anti-actin (1:1000; Sigma-Aldrich, St. Louis, MO). Horseradish peroxidase-conjugated secondary antibodies (1:10,000) were used. Blots were detected by ECL Plus (Amersham Biosciences, Piscataway, NJ).

Assessment of Apoptotic Cell Death

By Nuclear Morphology. Cells grown in chamber slides were treated as mentioned in the text or figure legends. Nuclei were stained with Hoechst 33342 (Molecular Probes) (1 μg/ml; 15 min at RT) and visualized under the fluorescent microscope (for UV excitation), and cells were scored as normal or apoptotic nuclei in several fields. At least 200 cells altogether in each treatment were counted and are shown as a percentage of cells with apoptotic nuclei among total cells counted.

By DNA Ladder Formation. Cells grown in a 10-cm culture dish were treated as mentioned above, harvested, and washed once with phosphate-buffered saline, and total DNA was isolated as described previously (Lee and Shacter, 1997). After digestion with proteinase K and RNase A, the DNA was separated in 2% agarose gels and visualized with ethidium bromide under UV light.

By Poly(ADP-Ribose) Polymerase (PARP) Cleavage/Caspase-3 Activation. PARP is a well known caspase-3 substrate. During apoptosis, caspase-3 is activated, so PARP cleavage can be used as a marker of apoptosis. Cells grown in a 10-cm culture dish were treated as described above and harvested, and total cell extracts were prepared. Equal amounts of proteins were separated in 4–12% acrylamide gels and immunoblotted with anti-PARP antibodies.

RESULTS

Knockdown of hFis1 or Drp1 Expression Induces Mitochondrial Fusion

Mitochondrial division in yeast requires at least seven to eight proteins (Dimmer *et al*., 2002), including Dnm1p (Otsuga *et al*., 1998; Bleazard *et al*., 1999) and Fis1p (Mozdy *et al*., 2000; Jakobs *et al*., 2003). The deletion or mutation of either of these genes disrupts proper mitochondrial division and causes mitochondrial membranes to form net-like structures (Dimmer *et al*., 2002). To explore the roles of the human orthologues of Dnm1p and Fis1p, Drp1 and hFis1, respectively, in mitochondrial fission and apoptosis, we "knocked down" their expression by using the short hairpin-activated gene silencing system (i.e., SHAGging; Cold Spring Harbor Laboratory) (Paddison *et al*., 2002). To generate cell lines that stably suppress the endogenous gene, we transferred the U6-shRNA inserts to pREP4, an episomally maintained mammalian expression vector with hygromycin as a selective marker.

Among 12 different oligonucleotides designed for hFis1 shRNA, only one, which corresponds to a sequence situated just outside of the 3′ end of the coding sequence, signifi-

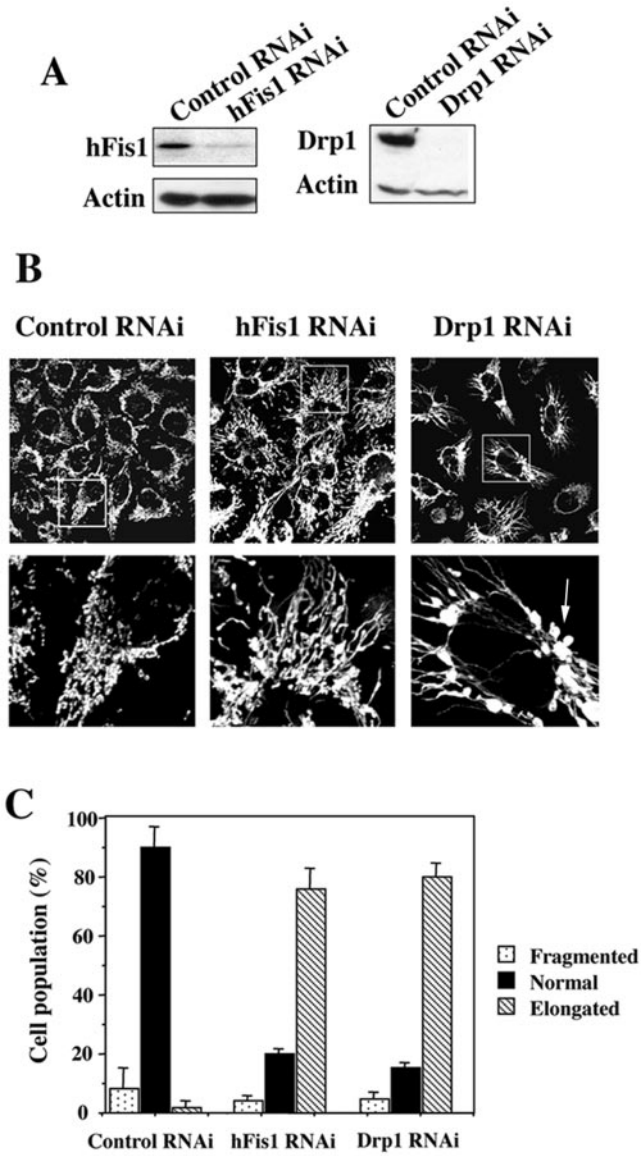

Figure 1. Knockdown of hFis1 or Drp1 expression induces mitochondrial fusion. HeLa cells were transfected with pREP4 constructs containing shRNA of the target sequence of hFis1, Drp1, or control, and the transfectants were selected by growth in media containing hygromycin B. (A) Total cell lysates from the hFis1 RNAi cells, Drp1 RNAi cells, and control RNAi cells were prepared, and the expression levels of hFis1 and Drp1 were analyzed by Western blotting. Actin level also was analyzed for a loading control. (B) Mitochondria of control RNAi cells, hFis1 RNAi cells, or Drp1 RNAi cells were visualized with Mitotracker Red CMXRos and analyzed by confocal microscopy. Enlargements are shown for detailed structure of mitochondria. An arrow shows a typical balloon-like structure in Drp1 RNAi cells. (C) Percentage of cell population with fragmented (dotted), normal (solid), or elongated (striped) mitochondria in control RNAi, hFis1 RNAi, or Drp1 RNAi culture. At least 200 cells in several fields were counted in each experiment. Data represent the mean ± SD of at least three independent experiments.

cantly inhibited hFis1 expression in HeLa cells. Selection of transfected HeLa cells with nearly complete depletion of hFis1 required ~1 wk of growth in the presence of hygromycin (Figure 1A). More than 70% of these cells had elongated mitochondria, whereas mitochondria in the remaining cells showed a more normal shape (short tubular) (Figure 1, B and C). Normal mitochondria in hFis1 RNAi cells might have been overscored, considering that hygromycin, which was used for the selection, tends to induce slightly shorter mitochondria (our unpublished data). Most of the cells that were transfected with a plasmid carrying control shRNA have normal relatively short tubular mitochondria and some fragmented ones, but never elongated mitochondria such as seen in hFis1 shRNA transfectants (Figure 1, B and C).

Unlike hFis1, four of six sequences targeted to Drp1 could silence Drp1 gene expression, including one reported previously to be effective in mammalian systems (Koch *et al*., 2003). On Drp1 depletion (Figure 1A) almost 80% of cells had elongated (fused) mitochondria (Figure 1, B and C). Even though mitochondria in hFis1 RNAi cells and Drp1 RNAi cells were both elongated extensively, the shapes of mitochondria were not the same. Many balloon-like or bulbed structures were seen at the base of tubules in the mitochondria of Drp1 RNAi cells but not hFis1 RNAi cells (Figure 1B, arrow). Interestingly, no differences in mitochondrial structure between *dnm*1Δ and *fis1*Δ cells were observed in yeast; both exhibited net-like structures (Mozdy *et al*., 2000). However, the larger size of mammalian mitochondria permits better visualization of morphology. Mammalian mitochondria have been reported to display expansions at the ends of mitochondria in cells overexpressing the dominant negative inhibitor Drp1^{K38A} (Smirnova *et al*., 2001).

Knockdown of hFis1 Did Not Affect the Distribution of Drp1 to Mitochondria

Drp1 is known not only to distribute predominantly to the cytosol but also accumulates at foci in the mitochondrial outer membrane that represent future fission sites (Labrousse *et al*., 1999; Smirnova *et al*., 2001). Because Drp1 lacks a mitochondrial targeting sequence, some protein(s) may be needed to recruit Drp1 to mitochondria. Human Fis1 is a good candidate for this recruitment because in yeast Fis1p is required for the proper assembly and distribution of Dnm1p-containing complexes on mitochondria (Mozdy *et al*., 2000; Tieu *et al*., 2002), and the structure of hFis1 resembles that of certain proteins involved in mitochondrial import (Suzuki *et al*., 2003). If this were the case, the mitochondrial distribution of Drp1 should be affected by hFis1 depletion. However, there was little or no difference in the Drp1 distribution between control RNAi cells and hFis1 RNAi cells assessed by immunocytochemistry (Figure 2A) or by Western blot analysis of the subcellular-fractionated S and HM (mostly mitochondrial fraction) samples (Figure 2B). Drp1 is distributed to the mitochondria in hFis1 RNAi cells to a similar extent as in control RNAi cells.

Fis1 Depletion Produces Greater Resistance to Apoptosis Than Depletion of Drp1

Overexpression of the dominant negative mutant Drp1^{K38A} induced mitochondrial fusion, and cells became resistant to apoptosis (Frank *et al*., 2001; Karbowski *et al*., 2002; Breckenridge *et al*., 2003), suggesting a close relationship between mitochondrial morphology and sensitivity to cell death. We examined how the knockdown of hFis1 expression affects the sensitivity to cell death by various apoptosis inducers and compared hFis1 RNAi cells to Drp1 RNAi cells. We found that <20% of hFis1 RNAi cells were apoptotic under conditions that produced 40–65% apoptosis of control RNAi cells (assessed by apoptotic nuclei) (Figure 3A). The caspase-3 activity of hFis1 RNAi cells from staurosporine (STS)-, actinomycin D (Act D)-, or anti-Fas–induced apoptosis was much lower than for control RNAi cells assessed by

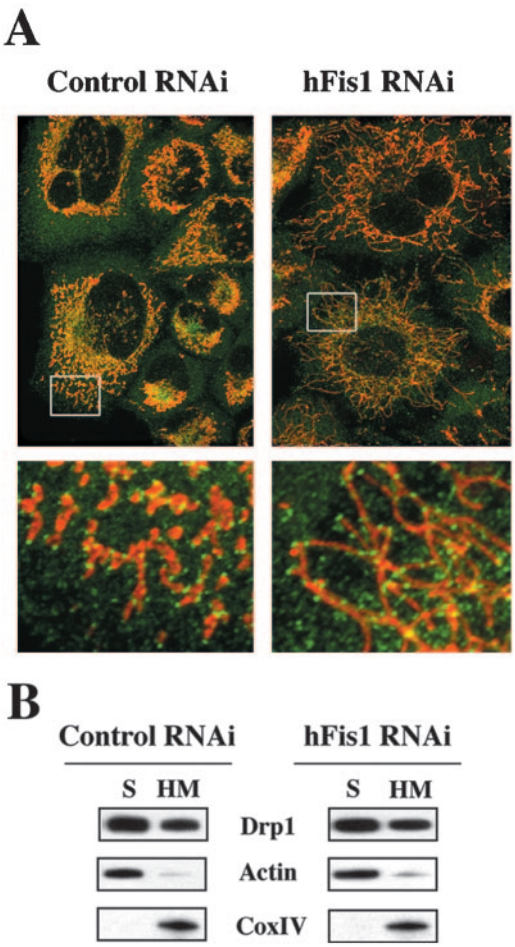

Figure 2. Knockdown of hFis1 did not affect the distribution of Drp1 to mitochondria. (A) Control or hFis1-depleted HeLa cells were incubated with Mitotracker CMXRos (red) for 20 min before fixation and stained with mouse monoclonal anti-DLP1/Drp1 followed by anti-mouse Alexa Fluor 488 antibodies (green). Mitochondria and distribution of Drp1 were analyzed by confocal microscopy. Red, mitochondria; green, Drp1. (B) HeLa cells depleted of hFis1 along with control RNAi were fractionated into S and HM (mainly mitochondria) and analyzed for the distribution of Drp1 by Western blotting. Fractionation quality was verified by the distribution of specific subcellular markers: CoxIV for mitochondria and actin for cytosol.

PARP cleavage (Figure 3B). Less inhibition of apoptosis by Drp1 silencing was observed (Figure 3, A and B).

To explore the mechanism of the cell death resistance of hFis1 RNAi cells, we examined two early events in apoptosis: the translocation of proapoptotic protein Bax from the cytosol to the mitochondria and the release of cytochrome *c* from the mitochondria to the cytosol (Kluck *et al*., 1997; Wolter *et al*., 1997). Control RNAi, hFis1 RNAi, and Drp1 RNAi cells were treated with actinomycin D in the presence of zVAD-fmk for 8 h, before Bax and cytochrome *c* staining by immunocytochemistry. As shown in Figure 4, A and B, most of the Bax in hFis1 RNAi cells was present in the cytosol and the cytochrome *c* localized to mitochondria under these conditions, in contrast to cells transfected with control RNAi. Interestingly, under the same conditions, in >80% of Drp1 RNAi cells Bax had translocated to mitochondria but in one-half of these cells, cytochrome *c* was still retained in the mitochondria (Figure 4, A and B). Typically, in healthy cells, Bax is localized in the cytosol and cytochrome *c* is in the mitochondria (Bax translocation negative and cytochrome *c* release negative), and upon apoptosis the Bax translocates to mitochondria and cytochrome *c* is released to the cytosol (Bax translocation positive and cytochrome *c* release positive). However, we observed an unusual population of Bax translocation positive- and cytochrome *c* release-negative cells during apoptosis of Drp1-depleted cells (Figure 4C), suggesting that Drp1 acts after Bax translocation to inhibit cytochrome *c* release. The results of immunocytochemistry were confirmed by Western blot analysis of the subcellular-fractionated S and HM samples (Figure 4D). In control RNAi cells, the majority of cytosolic Bax disappeared (translocated to the mitochondria), and more than one-half of the cytochrome *c* in mitochondria was released to the cytosol by actinomycin D treatment. In contrast, there was almost no difference in Bax or cytochrome *c* distribution in hFis1 RNAi cells with or without apoptosis induction. Thus, the absence of hFis1 blocked apoptosis upstream of Bax translocation. In Drp1 RNAi cells, however, cytosolic Bax disappeared almost completely, but cytochrome *c* release from the mitochondria was significantly lower than in control cells, indicating that the protection from apoptosis by Drp1 RNAi is downstream of Bax translocation and upstream of cytochrome *c* release. These results confirm the immunocytochemistry results and indicate that hFis1 and Drp1 work at different steps to promote apoptosis.

Overexpression of hFis1 Wild-Type (hFis1 wt) but Not C Terminus-truncated Mutant (hFis1 ΔC) Reverts the Apoptosis-resistant hFis1 RNAi Cells

To confirm that the apoptosis resistance in hFis1 RNAi cells is the result of hFis1 depletion, we reconstituted hFis1 expression in the hFis1 RNAi cells. The targeted sequence we used for hFis1 RNAi is situated just outside of the 3′ end of the coding sequence, so hFis1 cDNA constructs can be used to express hFis1 in the hFis1 RNAi cells. We cotransfected HeLa cells with cDNA constructs encoding either hFis1 wt or an hFis1ΔC mutant lacking the membrane anchor along with the hFis1 shRNAi construct, selected transfectants with hygromycin, and examined protein expression levels and sensitivity to apoptosis. As shown in Figure 5A, hFis1 (both wt and ΔC) was well expressed in the hFis1 RNAi cells (lanes 5–8). The hFis1 RNAi cells overexpressing hFis1 showed more sensitivity to apoptosis than hFis1 RNAi cells assessed by PARP cleavage (Figure 5A), nuclei fragmentation (Figure 5B), and cytochrome *c* release (Figure 5, C and D). However, the overexpression of hFis1 ΔC mutant in hFis1 RNAi cells did not affect the sensitivity to apoptosis. The results confirm that hFis1 is required for cell sensitivity to apoptosis and show that mitochondrial targeting of hFis1 is necessary for apoptosis promotion.

Knockdown of Opa1 Induces Mitochondrial Fragmentation and Sensitizes Cells to Apoptosis

The down-regulation of Opa1 in HeLa cells by RNAi was reported to lead to fragmentation of mitochondria, to the dissipation of the mitochondrial membrane potential, and to a disorganization of the cristae (Olichon *et al*., 2003). These events were followed by cytochrome *c* release and caspase-dependent apoptotic nuclear events. To study Opa1 function further, especially in conjunction with the fission proteins hFis1 and Drp1, we designed several shRNA constructs specific to the Opa1 sequence (coding and noncoding) for gene silencing by the same method we used for hFis1 and Drp1 RNAi. The sequence that was reported to down-regulate Opa1 (Olichon *et al*., 2003) also worked in the SHAGging system. A sequence that did not produce gene silencing was used as a control RNAi. It took 5–7 d after transfection for effective selection of transfectants, and Opa1 was almost completely depleted in this population (Figure 6A). The

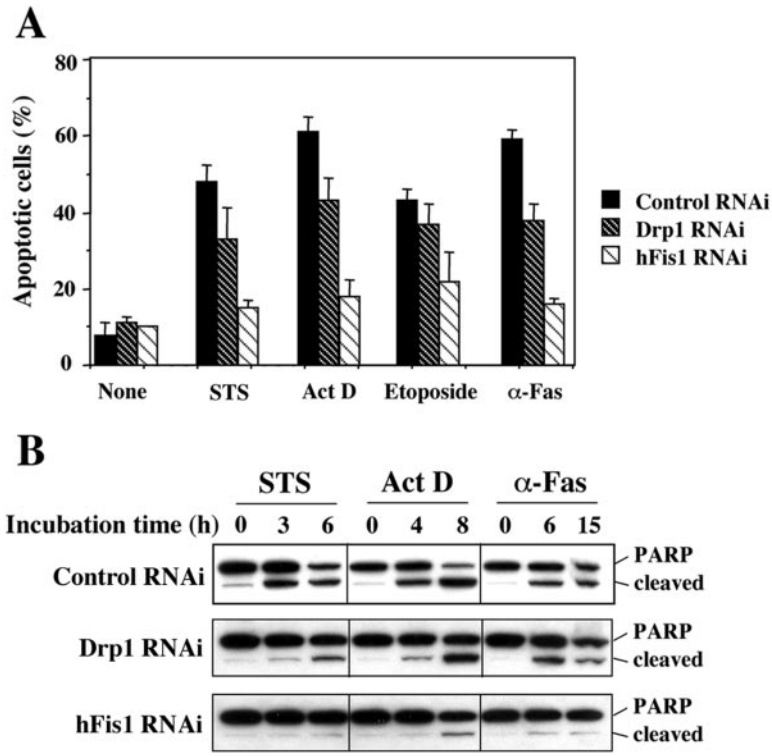

Figure 3. hFis1 depletion produces greater resistance to apoptosis than depletion of Drp1. (A) HeLa cells depleted of hFis1 or Drp1 by RNAi along with control RNAi cells were treated with STS (1 μM; 6 h), Act D (10 μM; 8 h), etoposide (100 μM; 30 h), or anti-Fas antibody (500 ng/ml, 15 h), and the nuclei were stained with Hoechst 33342 (1 μg/ml; 15 min at RT). Normal or apoptotic nuclei of these cells in several fields were counted under the fluorescent microscope (for UV excitation). At least 200 cells altogether in each treatment were counted and shown as a percentage of cells with apoptotic nuclei among total cells counted. The data are plotted as the mean $\pm$ SD of at least three independent experiments. (B) PARP cleavage was analyzed in the total extracts from HeLa cells depleted of hFis1, Drp1, and control, which were treated with STS (1 μM; 0, 3, 6 h), Act D (10 μM; 0, 4, 8 h), or anti-Fas (500 ng/ml; 0, 6, 15 h). The figure is a representative of at least three independent experiments.

lower band, which did not disappear, may be a nonspecific band rather than one of the eight alternative splicing variants (Delettre *et al*., 2000) because the targeting sequence we used for RNAi exists in all the splicing variants. Under these conditions, almost all the cells displayed extensively fragmented mitochondria, clearly different from the control RNAi cells (Figure 6, B and C).

In contrast to hFis1 and Drp1 RNAi cells, Opa1 RNAi cells are more sensitive to apoptosis induced by various stimuli compared with the control RNAi cells, and consistent with a previous report (Olichon *et al*., 2003), a portion of the cells (~25–35%) die spontaneously (Figure 6D). Opa1 down-regulated cells die with the typical hallmarks of apoptosis. Nuclear fragmentation (Figure 6D), DNA ladder formation (Figure 6E), Bax translocation, cytochrome *c* release (Figure 6, F and G), and caspase activation/PARP cleavage (Figure 6H) were all observed. The cell death caused by Opa1 depletion was inhibited by the general caspase inhibitor zVAD-fmk and by Bcl-2 overexpression (our unpublished data).

Cells Depleted of Both hFis1 and Opa1 Show Apoptosis Resistance in Spite of Extensive Mitochondrial Fragmentation

The down-regulation of hFis1 caused extensive mitochondrial fusion, and the cells became apoptosis resistant (Figures 1 and 3). In contrast, Opa1 down-regulation caused extensive mitochondrial fragmentation, and cells became more sensitive to death (Figure 6). In yeast, the elimination of fission mediators can be offset by eliminating fusion mediators (Sesaki and Jensen, 1999; Mozdy *et al*., 2000; Wong *et al*., 2000; Sesaki *et al*., 2003). Thus, we down-regulated both hFis1 and Opa1 and examined the effect on mitochondrial morphology and cell sensitivity to apoptosis.

More than 70% of the cells with both hFis1 and Opa1 almost completely depleted (hFis1/Opa1 RNAi) (Figure 7A) displayed fragmented mitochondria (Figure 7B), similar to results when cells were treated with Opa1 RNAi alone (Figure 6, B and C). This may reflect the rate of disappearance of Opa1 and hFis1 over the 5-d selection period. Therefore, Fis1 was depleted for 5 d and then Opa1 RNAi was transfected into the Fis1-depleted cells. Examining mitochondrial morphology 2 d after the Opa1 depletion showed fragmentation of the mitochondria in contrast to cells that expressed control RNAi in the second transfection (Figure 7C). Thus, even after depletion of hFis1 with RNAi, a finite rate of mitochondrial fission occurs that becomes predominant in the absence of Opa1. Slower but finite mitochondrial fission also occurs after genetic deletion of Fis1 in yeast (Jakobs *et al*., 2003). Residual fission of mitochondria in hFis/Opa1 RNAi was further confirmed by the results obtained using a mitochondrial fusion assay based on the measurement of dilution rates of mito-PAGFP, as described previously (Karbowski *et al*., 2004). We found complete inhibition of mitochondria fusion in hFis1/Opa1 double RNAi cells, indistinguishable from that detected in single Opa1 RNAi cells (Figure 7, D and E).

hFis1/Opa1 RNAi cells were very resistant to apoptosis, almost to the same extent as hFis1 RNAi cells and opposite from Opa1 RNAi cells (Figure 8A). However, the degree of the resistance of these cells varied substantially from experiment to experiment (shown by the larger SE bars in Figure 8A). When the hFis1/Opa1 RNAi cells and hFis1 RNAi cells (along with control RNAi cells and Opa1 RNAi cells) were treated longer with anti-Fas antibody, the difference in sensitivity to apoptosis between them became larger (Figure 8B). The hFis1/Opa1 RNAi cells are more sensitive than the hFis1 RNAi cells, but never as sensitive as the control RNAi cells or the Opa1 RNAi cells. The resistance of hFis1/Opa1 RNAi cells to apoptosis also was confirmed by inhibition of Act D-induced cytochrome *c* release and Bax translocation (Figure 8C). Opa1 is known to be associated with the inner mitochondrial membrane, and it has been reported that the depletion of Opa1 caused a loss in mitochondrial membrane potential (Olichon *et al*., 2003). Indeed, mitochondrial mem-

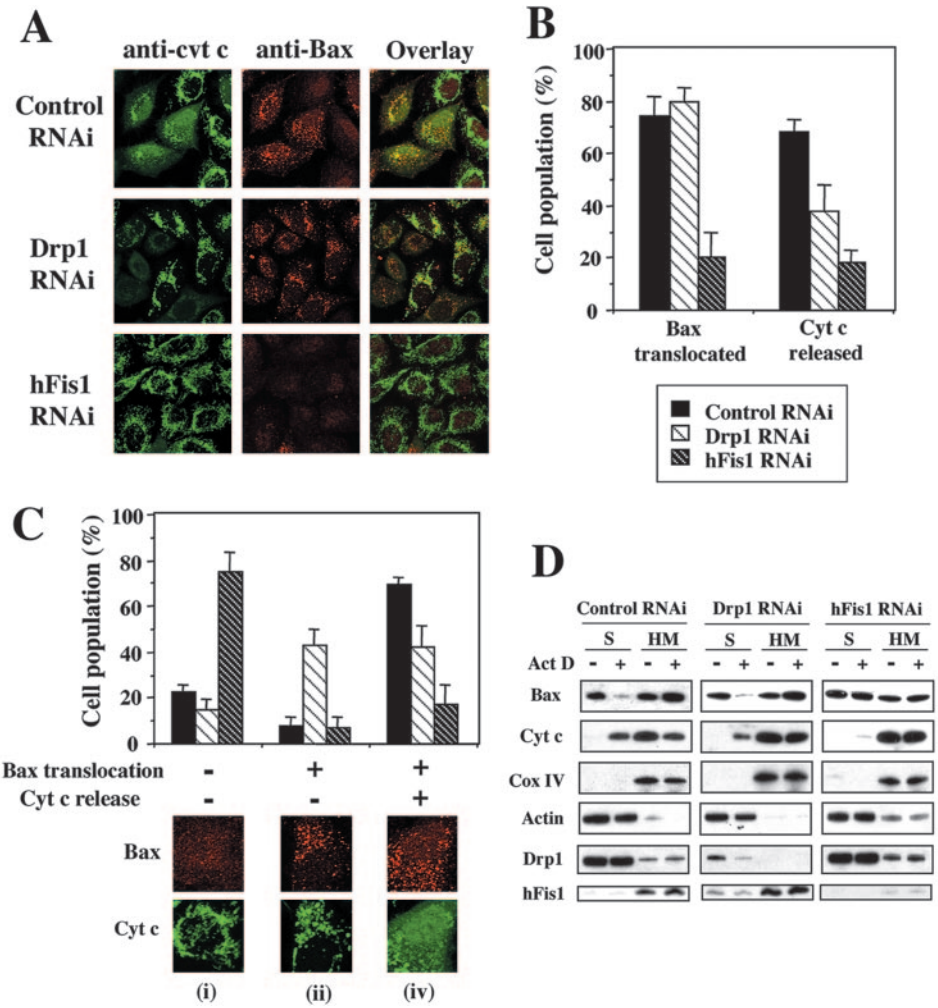

Figure 4. Both Bax translocation and cytochrome *c* release induced by actinomycin D are inhibited in hFis1-depleted HeLa cells, whereas cytochrome *c* release, but not Bax translocation, is inhibited in Drp1-depleted cells. (A) HeLa cells depleted of hFis1 or Drp1 by RNAi along with control RNAi cells were treated with Act D (10 μM; 8 h) in the presence of zVAD-fmk (50 μM), fixed, and double stained with anti-Bax (rabbit polyclonal, red) and anti-cytochrome *c* (mouse monoclonal, green) antibodies. (B) The number of cells displaying Bax translocation or cytochrome *c* release was counted and plotted as a percentage of total cells counted in each RNAi cell population that had been treated with Act D and stained with anti-Bax and anti-cytochrome *c* (the same samples as shown in A). At least 200 cells were counted altogether in several fields. Data are plotted as the mean ± SD of at least three independent experiments. (C) A unique group of cells (Bax had translocated but cytochrome *c* was not released) was seen in Drp1 RNAi cells. Four groups of cells were counted in each RNAi cell population that had been treated with Act D (the same samples as in A): i) Bax did not translocate and cytochrome *c* was not released; ii) Bax translocated, but cytochrome *c* is not released; iii) Bax not translocated, but cytochrome *c* is released; and iv) Bax translocated and cytochrome *c* is released were plotted as a percentage of total cells counted in each RNAi cell population. There were no cells categorized as iii, so only i, ii, and iv were plotted. Bars are labeled solid or striped, as in B. Data were plotted as the mean ± SD of at least three independent experiments. (D) HeLa cells depleted of Drp1 or hFis1 along with control RNAi were incubated with or without Act D (10 μM) for 8 h, fractionated into S and HM (mainly mitochondria), and analyzed for the distribution of Bax and cytochrome *c* by Western blotting. Fractionation quality was verified by the distribution of specific subcellular markers: CoxIV for mitochondria and actin for cytosol. To confirm the depletion of proteins (hFis1 and Drp1) and their localizations, hFis1 and Drp1 also were examined. The figure shown is representative of three independent experiments.

brane potential was lost in most of the Opa1-depleted cells, but the loss was prevented by hFis1 codepletion (Figure 8D). Thus, hFis1 is required for both the spontaneous and induced apoptosis caused by loss of Opa1 and functions epistatically to Opa1 in the apoptotic pathway.

DISCUSSION

Mitochondria fragment into smaller and more numerous units when mammalian cells are stimulated to undergo apoptosis (Mancini *et al.*, 1997; De Vos *et al.*, 1998; Zhuang *et al.*, 1998; Desagher *et al.*, 1999; Frank *et al.*, 2001; Karbowski *et al.*, 2002). When mitochondrial fission is blocked by overexpression of a dominant negative mutant of Drp1 ($Drp1^{K38A}$), the downstream events of mitochondrial-induced cell death, such as cytochrome *c* release, also are blocked, suggesting that mitochondrial fission might be a required step in apoptosis (Frank *et al.*, 2001; Breckenridge *et al.*, 2003). Bax, a proapoptotic Bcl-2 family member, colocalizes with Drp1 in mitochondrial foci (Karbowski *et al.*, 2002). On apoptosis initiation, Bax translocates from the cytosol to focal structures on the outer membrane of mitochondria (Nechushtan *et al.*, 2001; Valentijn *et al.*, 2003) that become sites of organelle scission (Karbowski *et al.*, 2002), suggesting that Bax may activate the mitochondrial fission machinery.

Screening yeast for mutants that suppress the phenotype of cells lacking the mitochondrial fusion gene FZO1 led to the initial identification of the importance of the outer mitochondrial membrane protein Fis1 in mitochondrial fission (Mozdy *et al.*, 2000; Tieu and Nunnari, 2000). To further explore the connection between mitochondrial morphology and apoptosis, we tested the role in apoptosis of another protein involved in mitochondrial fission, hFis1. Human Fis1 has been reported to induce mitochondrial fragmentation upon overexpression (James *et al.*, 2003; Yoon *et al.*, 2003), and loss of hFis1 induces elongation of mammalian mitochondria (Stojanovski *et al.*, 2004), suggesting a conserved role of *FIS1* in eukaryotes. In yeast, *FIS1* has been shown genetically to interact with *DNM1* and seems to be essential for the recruitment of Dnm1p (Drp1) into focal structures on mitochondria (Mozdy *et al.*, 2000; Tieu *et al.*, 2002). Although human Fis1 can be cross-linked to Drp1

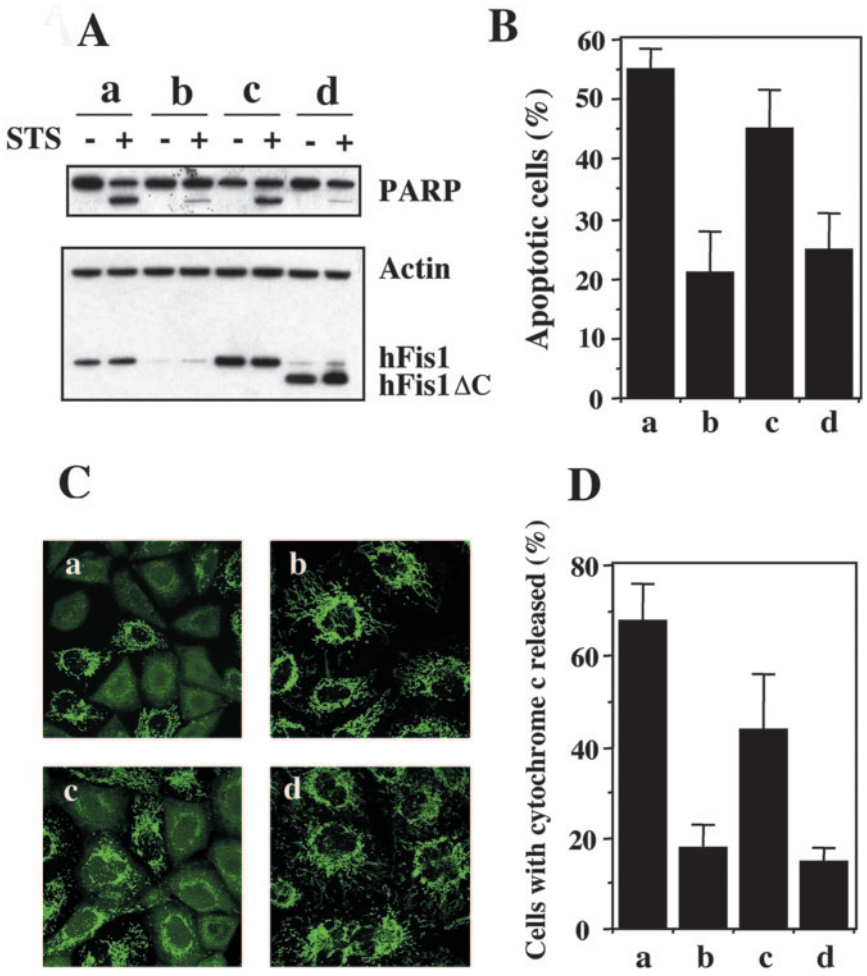

Figure 5. Overexpression of hFis1 wild-type (hFis1 wt) but not C terminus-truncated mutant (hFis1 ΔC) reverts apoptosis-resistant hFis1 RNAi cells. HeLa cells were transfected with control shRNA/pREP4 (a), hFis1 shRNA/pREP4 (b), hFis1 shRNA/pREP4 plus hFis1wt cDNA/pcDNA3.1 (c), or hFis1 shRNA/pREP4 plus hFis1ΔC cDNA/pcDNA3.1 (d), and transfectants were selected as described in *Materials and Methods*. (A) Transfectants of each group (a–d) were treated with or without STS (1 μM) for 6 h, lysed, and analyzed for hFis1 expression levels and PARP cleavage by Western blotting. Actin also was analyzed as a loading control. (B) Transfectants of each group (a–d) were treated with STS (1 μM; 6 h), and the nuclei were stained with Hoechst 33342 (1 μg/ml; 15 min at RT). Normal or apoptotic nuclei of these cells in several fields were counted under the fluorescent microscope (for UV excitation). At least 200 cells altogether in each treatment were counted and shown as a percentage of cells with apoptotic nuclei among the total cells counted. The data are plotted as the mean ± SD of at least three independent experiments. (C) Transfectants of each group (a–d) were treated with Act D (10 μM; 8 h) in the presence of zVAD-fmk (50 μM), fixed, and stained with anti-cytochrome *c* (mouse monoclonal, green) antibodies, and images were captured by confocal microscopy. (D) The number of cells whose cytochrome *c* was released was counted and plotted as a percentage of the total cells counted in each group (a–d) of transfectants that had been treated with Act D and stained with anti-cytochrome *c* (the same samples as shown in C). At least 200 cells were counted altogether in several fields. Data are plotted as the mean ± SD of at least three independent experiments.

(Yoon *et al*., 2003), the two do not seem to stably associate (James *et al*., 2003) nor does overexpression of hFis1 increase Drp1 binding to mitochondria (Suzuki *et al*., 2003). Here, we further show that, in contrast to yeast, loss of hFis1 does not decrease Drp1 binding to mitochondria (Figure 2, A and B). However, it is intriguing that hFis1 is required for Bax recruitment into the same Drp1-containing foci.

We have found that loss of hFis1 inhibits induction of apoptosis. Previously, it was reported that overexpression of hFis1 induced cell death that was inhibited by Bcl-xL overexpression (James *et al*., 2003). Interestingly, the apoptosis induced by hFis1 overexpression was not inhibited by the dominant negative inhibitor $Drp1^{K38A}$, whereas cytochrome *c* release in those cells was blocked. This correlates with our results that hFis1 and Drp1 work at different steps in the apoptosis pathway. Loss of hFis1 inhibits Bax translocation, whereas loss of Drp1 does not. Loss of Drp1, however, prevents cytochrome *c* release even in cells where Bax has translocated to mitochondria (Figure 4). This represents a novel step in apoptosis inhibition. Typically, Bax translocates to mitochondria very close in time to cytochrome *c* release so that, within a population, cells exist primarily as Bax translocation negative and cytochrome *c* release negative or Bax translocation positive and cytochrome *c* release positive. On loss of Drp1, a large proportion of the cells become Bax translocation positive and cytochrome *c* release negative, showing a new stage of apoptosis inhibition. In accordance with James *et al*. (2003), we find that loss of Drp1 produces a more significant inhibition of cytochrome *c* release than inhibition of apoptosis, hinting that Bax translocation may induce cell death independent of cytochrome *c* release. Other inhibitors of apoptosis such as Bcl-2 and the loss of hFis1 block both steps, whereas the general caspase inhibitor z-Val-Ala-Asp(OMe)-fluoromethyl ketone (zVAD-fmk) blocks neither, only inhibiting events downstream of outer mitochondrial membrane permeabilization. Thus, Drp1 seems to function subsequent to Bax translocation in the cytochrome *c* release process that occurs during apoptosis.

How does hFis1 act as a proapoptotic protein? The hFis1 structure (Suzuki *et al*., 2003) shows that the protein contains four tandem structures resembling the TPR. The TPR motifs are known to facilitate specific protein–protein interactions (Blatch and Lassle, 1999), suggesting that hFis1 may bind to other proteins and function as a molecular adaptor (receptor) on the mitochondrial outer membrane. TPR proteins in the outer mitochondrial membrane in addition to hFis1 include Tom20 (Iwahashi *et al*., 1997) and Tom70 (Young *et al*., 2003), both of which are involved in recruitment of other proteins to mitochondria. Although hFis1 does not seem to recruit Drp1 to mitochondria, a number of other interesting candidates will be worth examining. The notable differences between yeast and human mitochondrial fission and fusion machinery may offer insights into apoptosis as well as the mechanism of mitochondrial biogenesis.

Loss of a protein involved in mitochondrial fusion had the opposite effect on apoptosis from the loss of two proteins involved in mitochondrial fission. When Opa1 was depleted by RNAi, the mitochondria were extensively fragmented, and cells became

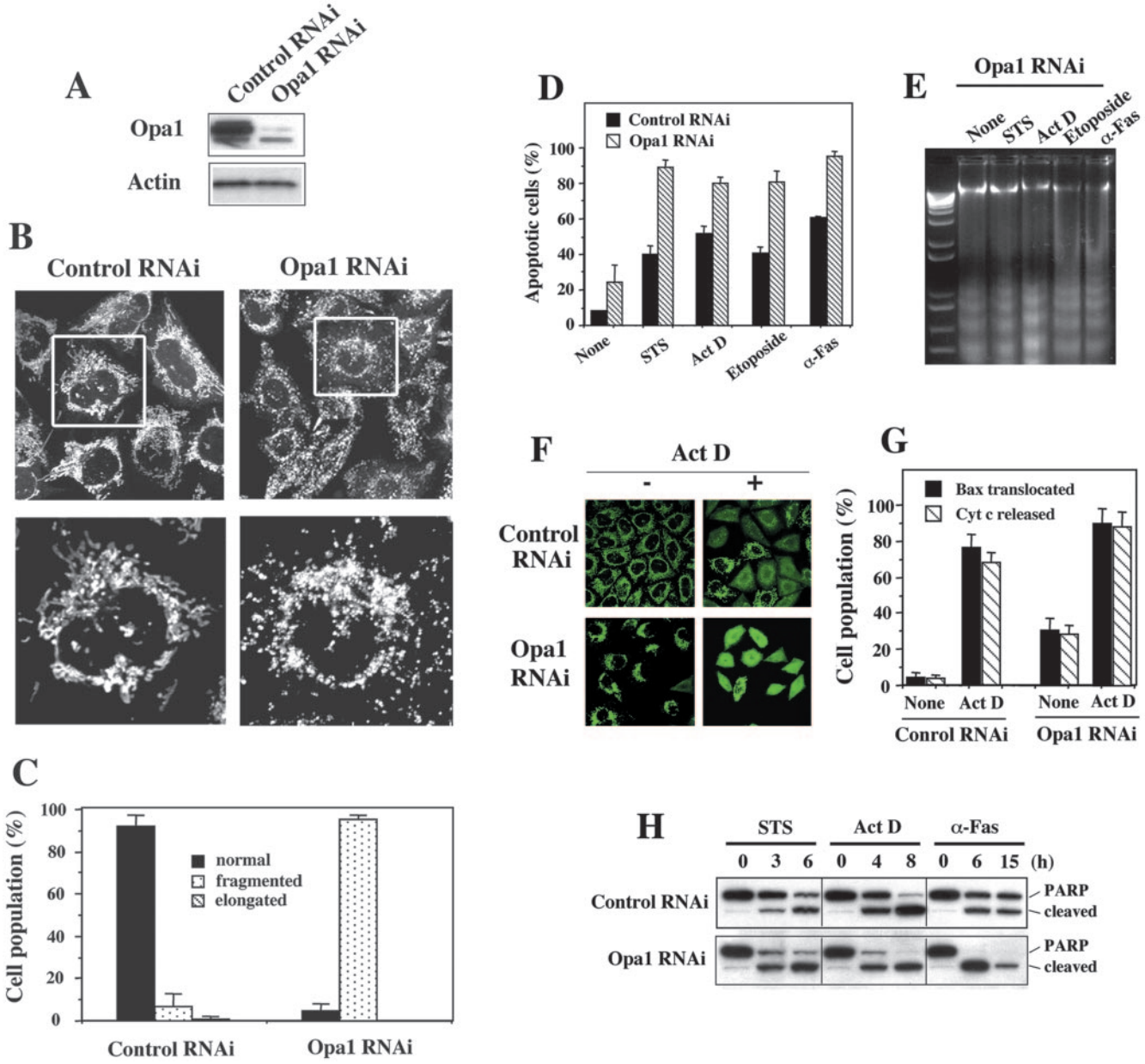

Figure 6. Depletion of Opa1 induces mitochondrial fragmentation, and cells become very sensitive to apoptosis. HeLa cells were transfected with pREP4 constructs containing shRNA of the target sequence of Opa1 or control, and the transfectants were selected by growing in media containing hygromycin B. (A) total cell lysates from the Opa1 RNAi cells along with control RNAi cells were prepared and the expression level of Opa1 was analyzed by Western blotting. Actin level also was analyzed as a loading control. (B) Mitochondria of control RNAi cells and Opa1 RNAi cells were visualized with Mitotracker Red CMXRos and analyzed by confocal microscopy. Enlargements are shown for detailed structure of mitochondria. (C) Percentage of cell population with fragmented (dotted), normal (solid), or elongated (striped) mitochondria in control RNAi or Opa1 RNAi culture. At least 200 cells in several fields were counted in each experiment. Data represent the mean ± SD of at least three independent experiments. (D) Opa1-depleted cells along with control RNAi cells were treated with STS (1 μM; 6 h), Act D (10 μM; 8 h), etoposide (100 μM; 30 h), or anti-Fas antibody (500 ng/ml; 15 h), and apoptotic nuclei (stained with Hoechst) were scored and plotted as a percentage of total cells (at least 200 cells) counted. Data are shown as the mean ± SD of three independent experiments. (E) Total DNA was isolated from the cells treated as described above and analyzed by agarose gel electrophoresis and visualized with ethidium bromide. The first lane is a DNA ladder control. The figure shown is a representative of three independent experiments. (F) HeLa cells depleted of Opa1 along with control RNAi cells were incubated with or without Act D (10 μM) for 8 h in the presence of zVAD-fmk, fixed, and stained with anti-Bax (red; our unpublished data) and anti-cytochrome *c* antibodies (green). (G) The number of cells in F displaying Bax translocation or cytochrome *c* release was counted and plotted as a percentage of total cells counted in each RNAi cell population that had been treated with or without Act D and stained with anti-Bax and anti-cytochrome *c* antibodies (the same samples as shown in F). At least 200 cells were counted altogether in several fields. Data are plotted as the mean ± SD of at least three independent experiments. (H) PARP cleavage was analyzed in the total extracts from HeLa cells depleted of Opa1 and control that were treated with STS (1 μM; 0, 3, 6 h), Act D (10 μM; 0, 4, 8 h), or anti-Fas (500 ng/ml; 0, 6, 15 h). The figure is a representative of at least three independent experiments.

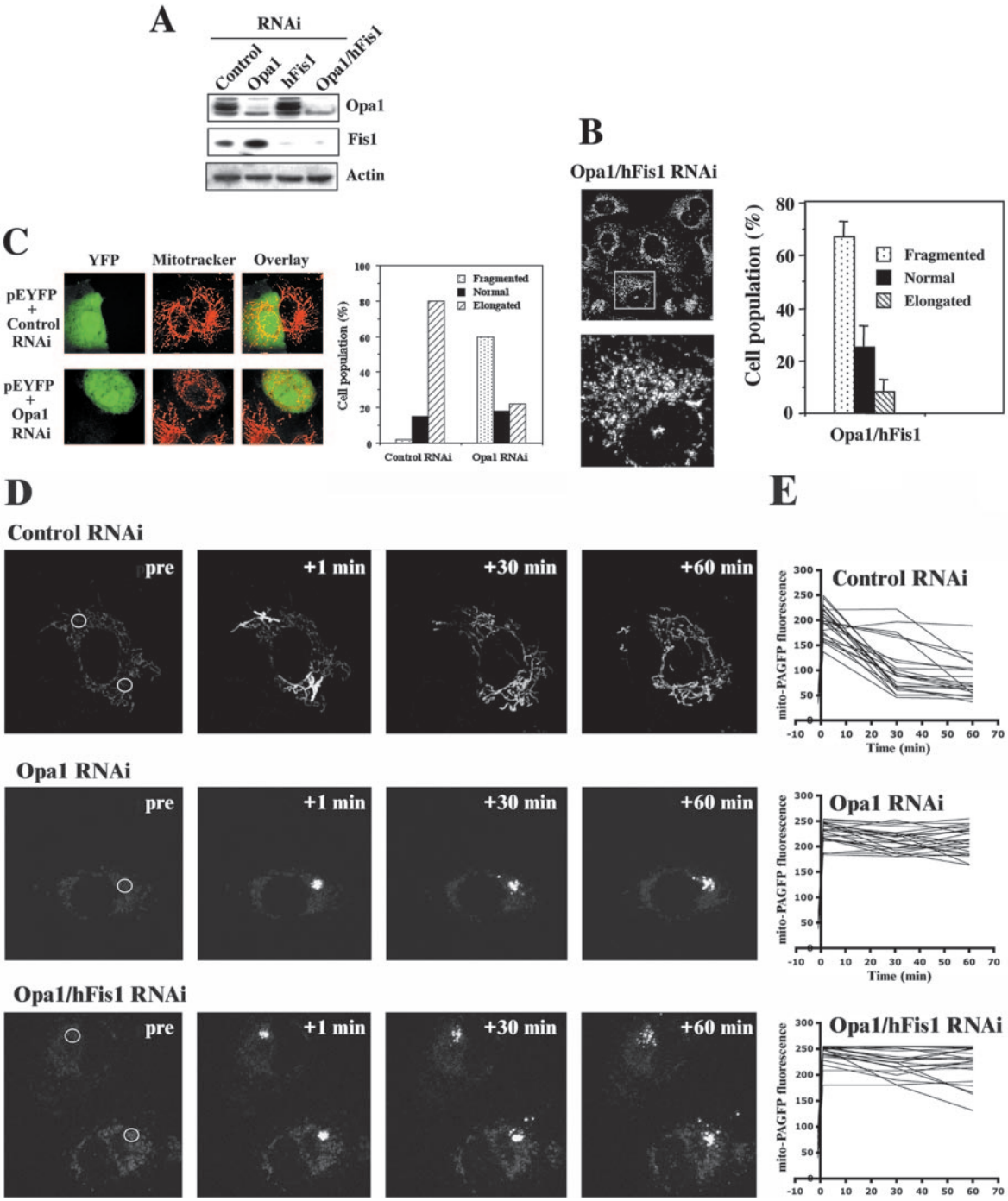

Figure 7. Mitochondria are extensively fragmented in the cells depleted of both hFis1 and Opa1. HeLa cells were transfected with pREP4 constructs containing shRNA of the target sequence of hFis1, Opa1, or both of them together along with control, and the transfectants were selected by growing in media containing hygromycin B. (A) Total cell lysates from the hFis1 RNAi cells, Opa1 RNAi cells, or both hFis1 and Opa1 RNAi cells along with control RNAi cells were prepared, and the expression levels of hFis1 and Opa1 were analyzed by Western blotting. Actin also was analyzed as a loading control. (B) Left, mitochondria of hFis1/Opa1 RNAi cells were visualized with Mitotracker Red CMXRos and analyzed by confocal microscopy. An enlargement is shown for detailed structure of mitochondria. Right, percentage of cell population with fragmented (dotted), normal (solid), or elongated (striped) mitochondria in hFis1/Opa1 RNAi cell culture. At least 200 cells in several fields were counted in each experiment. Data represent the mean ± SD of at least three independent experiments. (C) The elongated mitochondrial morphology in hFis1-depleted cells was reversed by subsequent depletion of Opa1. Hela cells depleted of hFis1 by RNAi were selected for 5 d and transfected again with Opa1 shRNA- or a control shRNA-construct and examined 2 d later. To identify transfectants, pEYFP vector was cotransfected. Mitochondria were visualized with Mitotracker Red CMXRos and analyzed by confocal microscopy. (D and E) Control RNAi, Opa1 RNAi, and hFis1/Opa1 RNAi double RNAi cells were analyzed for mitochondrial fusion by using mito-PAGF–based fusion assay. Cells were transfected with mito-PAGFP, followed by the photoactivation of the small regions within the cells (white circles in prepanels) and confocal acquisition of z-series covering the entire thickness of the cell. (E) Changes in the fluorescence intensity within activated regions were measured over time.

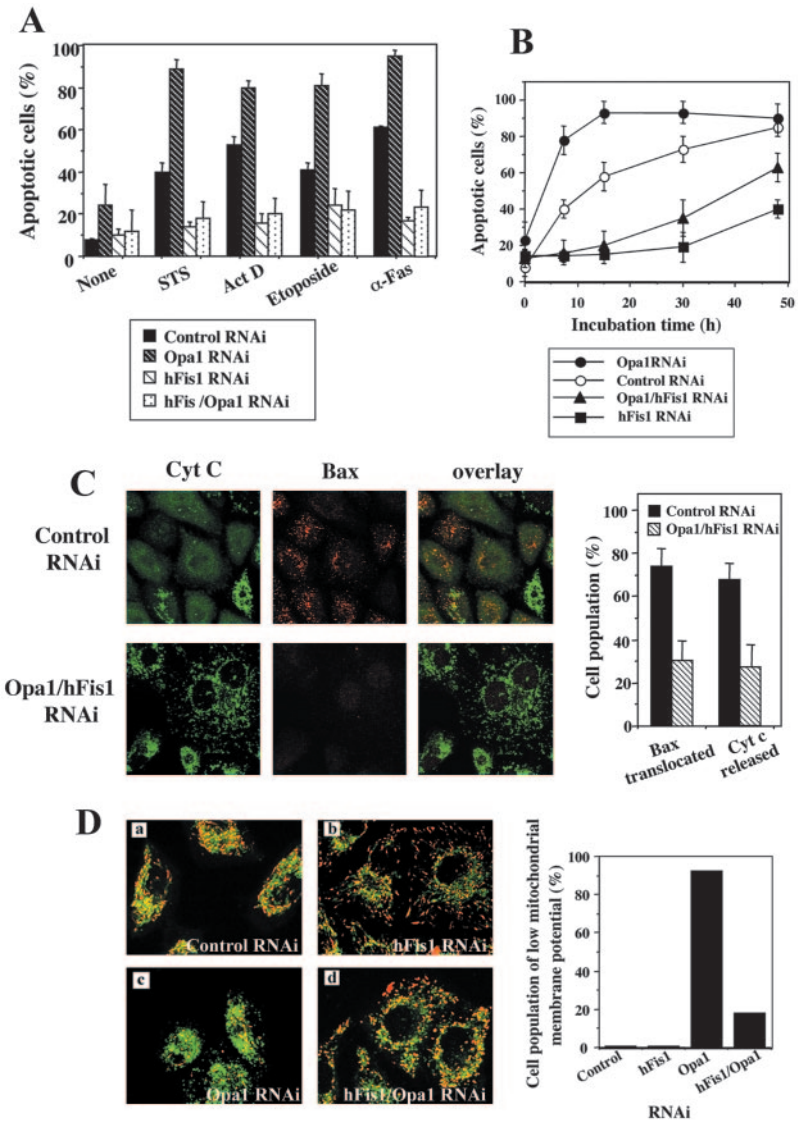

Figure 8. Cells depleted of both hFis1 and Opa1 show apoptosis resistance like hFis1-depleted cells. (A) HeLa cells depleted of hFis1, Opa1, or both of them by RNAi along with control RNAi cells were treated with STS (1 μM; 6 h), Act D (10 μM; 8 h), etoposide (100 μM; 30 h), or anti-Fas antibody (500 ng/ml; 15 h), and the nuclei were stained with Hoechst 33342 (1 μg/ml; 15 min at RT). Normal or apoptotic nuclei of these cells in several fields were counted under the fluorescent microscope (for UV excitation). At least 200 cells altogether in each treatment were counted and plotted as a percentage of cells with apoptotic nuclei among the total cells counted. The data are shown as the mean ± SD of at least three independent experiments. (B) HeLa cells depleted of Opa1, hFis1, or both of them along with control RNAi cells were incubated with anti-Fas antibody (500 ng/ml) for the periods as indicated, and the nuclei were stained and counted as normal or apoptotic nuclei. At least 200 cells altogether were counted in each sample at each time point and plotted as a percentage of cells with apoptotic nuclei among the total cells counted. The data were plotted as the mean ± SD of at least three independent experiments. (C) Bax translocation and cytochrome *c* release induced by Act D treatment are inhibited in hFis/Opa1 RNAi cells. Left, HeLa cells depleted of both hFis1 and Opa1 by RNAi along with control RNAi cells were treated with Act D (10 μM; 8 h) in the presence of zVAD-fmk (50 μM), fixed, and double stained with anti-Bax (rabbit polyclonal, red) and anti-cytochrome *c* (mouse monoclonal, green) antibodies. Right, the number of cells displaying Bax translocation or cytochrome *c* release was counted and plotted as a percentage of the total cells counted in each RNAi cell population that had been treated with Act D and stained with anti-Bax and anti-cytochrome *c* antibodies (the same samples as shown on the left). At least 200 cells were counted altogether in several fields. Data are plotted as the mean ± SD of at least three independent experiments. (D) hFis1 depletion prevents mitochondrial membrane potential reduction induced by Opa1 depletion. Left, HeLa cells depleted of hFis1 (b), Opa1 (c), or both of them (d) along with control RNAi cells (a) were incubated with 5 μg/ml JC-1 for 20 min and observed by confocal microscopy. JC-1 is a cationic dye that indicates mitochondrial polarization by shifting its fluorescence emission from green to red. Regions of high mitochondrial membrane potential are indicated by red fluorescence, and regions of low mitochondrial membrane potential are indicated by green fluorescence. Right, the number of cells with mitochondria whose membrane potential was lost was counted and plotted as a percentage of the total cells counted in each RNAi cell population.

very sensitive to apoptosis, consistent with the results reported by others (Olichon *et al*., 2003; Griparic *et al*., 2004), and further correlating mitochondrial fragmentation with sensitivity to apoptosis. Our results show that wild-type Opa1 may function normally as an antiapoptotic protein, keeping spontaneous apoptosis in check. However, if hFis1 is down-regulated, cells do not require Opa1 to prevent apoptosis, suggesting that Opa1 may be normally counteracting the proapoptotic action of hFis1. Thus, although mitochondrial fragmentation per se does not necessarily result in apoptosis, the components of the mitochondrial fission-fusion machinery can positively and negatively regulate apoptosis, and the rate of mitochondrial fission and fusion may be directly connected to the process of programmed cell death.

ACKNOWLEDGMENTS

We thank Dr. Craig Blackstone (National Institute of Neurological Disorders and Stroke/National Institutes of Health) for providing antibodies against Opa1 and for critical reading of the manuscript and many useful suggestions. We also thank Drs. Sang-Joon Park and Hyeog Kang (National Heart, Lung, and Blood Institute/National Institutes of Health) for much advice on the RNAi experiments. This work was supported by the intramural program of the National Institute of Neurological Disorders and Stroke/National Institutes of Health.

REFERENCES

Alexander, C., *et al*. (2000). OPA1, encoding a dynamin-related GTPase, is mutated in autosomal dominant optic atrophy linked to chromosome 3q28. Nat. Genet. *26*, 211–215.

Bereiter-Hahn, J. (1990). Behavior of mitochondria in the living cell. Int. Rev. Cytol. *122*, 1–63.

Blatch, G.L., and Lassle, M. (1999). The tetratricopeptide repeat: a structural motif mediating protein-protein interactions. Bioessays *21*, 932–939.

Bleazard, W., McCaffery, J.M., King, E.J., Bale, S., Mozdy, A., Tieu, Q., Nunnari, J., and Shaw, J.M. (1999). The dynamin-related GTPase Dnm1 regulates mitochondrial fission in yeast. Nat. Cell Biol. *1*, 298–304.

Breckenridge, D.G., Stojanovic, M., Marcellus, R.C., and Shore, G.C. (2003). Caspase cleavage product of BAP31 induces mitochondrial fission through

endoplasmic reticulum calcium signals, enhancing cytochrome c release to the cytosol. J. Cell Biol. *160*, 1115–1127.

Chen, H., Detmer, S.A., Ewald, A.J., Griffin, E.E., Fraser, S.E., and Chan, D.C. (2003). Mitofusins Mfn1 and Mfn2 coordinately regulate mitochondrial fusion and are essential for embryonic development. J. Cell Biol. *160*, 189–200.

De Vos, K., Goossens, V., Boone, E., Vercammen, D., Vancompernolle, K., Vandenabeele, P., Haegeman, G., Fiers, W., and Grooten, J. (1998). The 55-kDa tumor necrosis factor receptor induces clustering of mitochondria through its membrane-proximal region. J. Biol. Chem. *273*, 9673–9680.

Delettre, C., *et al*. (2000). Nuclear gene OPA1, encoding a mitochondrial dynamin-related protein, is mutated in dominant optic atrophy. Nat. Genet. *26*, 207–210.

Desagher, S., Osen-Sand, A., Nichols, A., Eskes, R., Montessuit, S., Lauper, S., Maundrell, K., Antonsson, B., and Martinou, J.C. (1999). Bid-induced conformational change of Bax is responsible for mitochondrial cytochrome c release during apoptosis. J. Cell Biol. *144*, 891–901.

Dimmer, K.S., Fritz, S., Fuchs, F., Messerschmitt, M., Weinbach, N., Neupert, W., and Westermann, B. (2002). Genetic basis of mitochondrial function and morphology in *Saccharomyces cerevisiae*. Mol. Biol. Cell *13*, 847–853.

Dohm, J.A., Lee, S.J., Hardwick, J.M., Hill, R.B., and Gittis, A.G. (2004). Cytosolic domain of the human mitochondrial fission protein fis1 adopts a TPR fold. Proteins *54*, 153–156.

Frank, S., Gaume, B., Bergmann-Leitner, E.S., Leitner, W.W., Robert, E.G., Catez, F., Smith, C.L., and Youle, R.J. (2001). The role of dynamin-related protein 1, a mediator of mitochondrial fission, in apoptosis. Dev. Cell *1*, 515–525.

Griparic, L., Van Der Wel, N.N., Orozco, I.J., Peters, P.J., and Van Der Bliek, A.M. (2004). Loss of the intermembrane space protein Mgm1/Opa1 induces swelling and localized constrictions along the lengths of mitochondria. J. Biol. Chem. *279*, 18792–18798.

Hinshaw, J.E. (2000). Dynamin and its role in membrane fission. Annu. Rev. Cell Dev. Biol. *16*, 483–519.

Ishihara, N., Jofuku, A., Eura, Y., and Mihara, K. (2003). Regulation of mitochondrial morphology by membrane potential, and DRP1-dependent division and FZO1-dependent fusion reaction in mammalian cells. Biochem. Biophys. Res. Commun. *301*, 891–898.

Iwahashi, J., Yamazaki, S., Komiya, T., Nomura, N., Nishikawa, S., Endo, T., and Mihara, K. (1997). Analysis of the functional domain of the rat liver mitochondrial import receptor Tom20. J. Biol. Chem. *272*, 18467–18472.

Jakobs, S., Martini, N., Schauss, A.C., Egner, A., Westermann, B., and Hell, S.W. (2003). Spatial and temporal dynamics of budding yeast mitochondria lacking the division component Fis1p. J. Cell Sci. *116*, 2005–2014.

James, D.I., Parone, P.A., Mattenberger, Y., and Martinou, J.C. (2003). hFis1, a novel component of the mammalian mitochondrial fission machinery. J. Biol. Chem. *278*, 36373–36379.

Karbowski, M., Arnoult, D., Chen, H., Chan, D.C., Smith, C.L., and Youle, R.J. (2004). Quantitation of mitochondrial dynamics by photolabeling of individual organelles shows that mitochondrial fusion is blocked during the Bax activation phase of apoptosis. J. Cell Biol. *164*, 493–499.

Karbowski, M., Lee, Y.J., Gaume, B., Jeong, S.Y., Frank, S., Nechushtan, A., Santel, A., Fuller, M., Smith, C.L., and Youle, R.J. (2002). Spatial and temporal association of Bax with mitochondrial fission sites, Drp1, and Mfn2 during apoptosis. J. Cell Biol. *159*, 931–938.

Kluck, R.M., Bossy-Wetzel, E., Green, D.R., and Newmeyer, D.D. (1997). The release of cytochrome c from mitochondria: a primary site for Bcl-2 regulation of apoptosis. Science *275*, 1132–1136.

Koch, A., Thiemann, M., Grabenbauer, M., Yoon, Y., McNiven, M.A., and Schrader, M. (2003). Dynamin-like protein 1 is involved in peroxisomal fission. J. Biol. Chem. *278*, 8597–8605.

Labrousse, A.M., Zappaterra, M.D., Rube, D.A., and van der Bliek, A.M. (1999). C. *elegans* dynamin-related protein DRP-1 controls severing of the mitochondrial outer membrane. Mol. Cell *4*, 815–826.

Lee, Y., and Shacter, E. (1997). Bcl-2 does not protect Burkitt's lymphoma cells from oxidant-induced cell death. Blood *89*, 4480–4492.

Mancini, M., Anderson, B.O., Caldwell, E., Sedghinasab, M., Paty, P.B., and Hockenbery, D.M. (1997). Mitochondrial proliferation and paradoxical membrane depolarization during terminal differentiation and apoptosis in a human colon carcinoma cell line. J. Cell Biol. *138*, 449–469.

Mozdy, A.D., McCaffery, J.M., and Shaw, J.M. (2000). Dnm1p GTPase-mediated mitochondrial fission is a multi-step process requiring the novel integral membrane component Fis1p. J. Cell Biol. *151*, 367–380.

Nechushtan, A., Smith, C.L., Lamensdorf, I., Yoon, S.H., and Youle, R.J. (2001). Bax and Bak coalesce into novel mitochondria-associated clusters during apoptosis. J. Cell Biol. *153*, 1265–1276.

Nunnari, J., Marshall, W.F., Straight, A., Murray, A., Sedat, J.W., and Walter, P. (1997). Mitochondrial transmission during mating in *Saccharomyces cerevisiae* is determined by mitochondrial fusion and fission and the intramitochondrial segregation of mitochondrial DNA. Mol. Biol. Cell *8*, 1233–1242.

Olichon, A., Baricault, L., Gas, N., Guillou, E., Valette, A., Belenguer, P., and Lenaers, G. (2003). Loss of OPA1 perturbates the mitochondrial inner membrane structure and integrity, leading to cytochrome c release and apoptosis. J. Biol. Chem. *278*, 7743–7746.

Olichon, A., *et al*. (2002). The human dynamin-related protein OPA1 is anchored to the mitochondrial inner membrane facing the inter-membrane space. FEBS Lett. *523*, 171–176.

Otsuga, D., Keegan, B.R., Brisch, E., Thatcher, J.W., Hermann, G.J., Bleazard, W., and Shaw, J.M. (1998). The dynamin-related GTPase, Dnm1p, controls mitochondrial morphology in yeast. J. Cell Biol. *143*, 333–349.

Paddison, P.J., Caudy, A.A., Bernstein, E., Hannon, G.J., and Conklin, D.S. (2002). Short hairpin RNAs (shRNAs) induce sequence-specific silencing in mammalian cells. Genes Dev. *16*, 948–958.

Santel, A., and Fuller, M.T. (2001). Control of mitochondrial morphology by a human mitofusin. J. Cell Sci. *114*, 867–874.

Satoh, M., Hamamoto, T., Seo, N., Kagawa, Y., and Endo, H. (2003). Differential sublocalization of the dynamin-related protein OPA1 isoforms in mitochondria. Biochem. Biophys. Res. Commun. *300*, 482–493.

Sesaki, H., and Jensen, R.E. (1999). Division versus fusion: Dnm1p and Fzo1p antagonistically regulate mitochondrial shape. J. Cell Biol. *147*, 699–706.

Sesaki, H., Southard, S.M., Yaffe, M.P., and Jensen, R.E. (2003). Mgm1p, a dynamin-related GTPase, is essential for fusion of the mitochondrial outer membrane. Mol. Biol. Cell *14*, 2342–2356.

Smirnova, E., Griparic, L., Shurland, D.L., and van der Bliek, A.M. (2001). Dynamin-related protein Drp1 is required for mitochondrial division in mammalian cells. Mol. Biol. Cell *12*, 2245–2256.

Smirnova, E., Shurland, D.L., Ryazantsev, S.N., and van der Bliek, A.M. (1998). A human dynamin-related protein controls the distribution of mitochondria. J. Cell Biol. *143*, 351–358.

Stojanovski, D., Koutsopoulos, O.S., Okamoto, K., and Ryan, M.T. (2004). Levels of human Fis1 at the mitochondrial outer membrane regulate mitochondrial morphology. J. Cell Sci. *117*, 1201–1210.

Suzuki, M., Jeong, S.Y., Karbowski, M., Youle, R.J., and Tjandra, N. (2003). The solution structure of human mitochondria fission protein Fis1 reveals a novel TPR-like helix bundle. J. Mol. Biol. *334*, 445–458.

Tieu, Q., and Nunnari, J. (2000). Mdv1p is a WD repeat protein that interacts with the dynamin-related GTPase, Dnm1p, to trigger mitochondrial division. J. Cell Biol. *151*, 353–366.

Tieu, Q., Okreglak, V., Naylor, K., and Nunnari, J. (2002). The WD repeat protein, Mdv1p, functions as a molecular adaptor by interacting with Dnm1p and Fis1p during mitochondrial fission. J. Cell Biol. *158*, 445–452.

Valentijn, A.J., Metcalfe, A.D., Kott, J., Streuli, C.H., and Gilmore, A.P. (2003). Spatial and temporal changes in Bax subcellular localization during anoikis. J. Cell Biol. *162*, 599–612.

Wolter, K.G., Hsu, Y.T., Smith, C.L., Nechushtan, A., Xi, X.G., and Youle, R.J. (1997). Movement of Bax from the cytosol to mitochondria during apoptosis. J. Cell Biol. *139*, 1281–1292.

Wong, E.D., Wagner, J.A., Gorsich, S.W., McCaffery, J.M., Shaw, J.M., and Nunnari, J. (2000). The dynamin-related GTPase, Mgm1p, is an intermembrane space protein required for maintenance of fusion competent mitochondria. J. Cell Biol. *151*, 341–352.

Yoon, Y., Krueger, E.W., Oswald, B.J., and McNiven, M.A. (2003). The mitochondrial protein hFis1 regulates mitochondrial fission in mammalian cells through an interaction with the dynamin-like protein DLP1. Mol. Cell. Biol. *23*, 5409–5420.

Young, J.C., Hoogenraad, N.J., and Hartl, F.U. (2003). Molecular chaperones Hsp90 and Hsp70 deliver preproteins to the mitochondrial import receptor Tom70. Cell *112*, 41–50.

Zhu, P.P., Patterson, A., Lavoie, B., Stadler, J., Shoeb, M., Patel, R., and Blackstone, C. (2003). Cellular localization, oligomerization, and membrane association of the hereditary spastic paraplegia 3A (SPG3A) protein atlastin. J. Biol. Chem. *278*, 49063–49071.

Zhuang, J., Dinsdale, D., and Cohen, G.M. (1998). Apoptosis, in human monocytic THP. 1 cells, results in the release of cytochrome c from mitochondria prior to their ultracondensation, formation of outer membrane discontinuities and reduction in inner membrane potential. Cell. Death Differ. *5*, 953–962.